

JPMTR-2312
DOI 10.14622/JPMTR-2312
UDC 539.6-033.5:519.8|53.08

Original scientific paper | 184
Received: 2023-09-14
Accepted: 2023-11-14

Static- and dynamic-wetting measurements on 3-aminopropyltriethoxysilane-functionalized float glass surfaces as a method for indicating adhesion forces

Sarah Patejdl, Ulrich Jung, Christopher Knoth and Patrick Görrn

Bergische Universität Wuppertal,
Gaußstraße 20, 42119 Wuppertal, Germany

patejdl@uni-wuppertal.de
ujung@uni-wuppertal.de

Abstract

Earlier research demonstrated the dependence of 3-aminopropyltriethoxysilane (APTES) wetting properties on cleaning, functionalization, and post-treatment processes on oxide surfaces, e.g., glass surfaces or Si wafer surfaces, but not on float glass surfaces. Also, oxide glass surfaces were functionalized by different silanes and were applied with ultraviolet (UV) radiation-curable inks or adhesives. The resulting adhesion forces differed depending on the silane and the UV-curable ink or adhesive used. The chemical diversity of silanes leads to different surface energy on glass surfaces and was used to gain further insights into a correlation between wetting properties and the resulting adhesion forces. This work investigates the suitability of dynamic contact angle measurement (DCA) for indicating adhesion forces via contact angle hysteresis and the resulting drop age. Two types of test fluids (diiodomethane and water) are applied on hydrophilic float glass surfaces (air side and tin side) and on a hydrophobic PE foil surface. The functionalization of glass substrates is realised by reproducible vapour and solution deposition of APTES, which results in different wetting properties of float glass surfaces. The investigations are complemented by static contact angle measurements of different test fluids, and the appropriate surface energies are evaluated via the Owens, Wendt, Rabel, and Kaelble method. The polar and non-polar surfaces are clearly differentiable by contact angle hysteresis and drop age. The DCA results of the hydrophilic float glass surfaces and the hydrophobic PE foil surface confirm the suitability of using the DCA parameters hysteresis and drop age for indicating adhesion forces on functionalized float glass surfaces. The hysteresis and drop age of assumed completely APTES-functionalized float glass surfaces confirm the suitability of the DCA measurement for indicating adhesion forces, too. The test fluid diiodomethane is suitable for indicating adhesion forces on the air side of the float glass, and the test fluid water is suitable for indicating adhesion forces on the tin side of the float glass. With the increased water contact angle, the hysteresis and drop age increased using the polar test fluid water. This does not support the polarity theory of de Bruyne. By using the non-polar test fluid diiodomethane, the hysteresis and drop age decrease with increasing contact angle and also do not support the adhesion theory of de Bruyne. The research results show a way of indicating the adhesion forces of different functionalized float glass surfaces, by using only one silane, and serves as a pre-step for better understanding of e.g. UV-ink adhesion forces dependent on glass surface wetting properties.

Keywords: dynamic contact angle, hysteresis, drop age, 3-aminopropyltriethoxysilane, adhesion

1. Introduction and background

Among trialkoxyorganosilanes, 3-aminopropyltriethoxysilane (APTES) is one of the best-known and most commonly widely used trialkoxyorganosilane for chemical and physical modification of oxide surfaces, e.g., microscope slides and Si-wafer surfaces, and is used as a coupling agent to promote adhesion between inorganic and organic substrates (Plueddemann, 1991;

Mittal and O'kane, 1976). According to Plueddemann (1970, p. 185) and Wolf (2022, p. 4) the APTES molecule follows the general formula of organosilanes $(X)_3Si(CH_2)_3Y$; while X marks the alkoxy group, e.g., methoxy or ethoxy group (OCH_3 , OC_2H_5), Y marks the organofunctional group, e.g., amino, vinyl, mercapto, etc., and CH_2 marks the alkylene bridge (called spacer or linker), typically a propylene chain. APTES has three hydrolyzable ethoxy groups and one organofunctional amino

group (NH₂) per molecule. The bonding of inorganic to organic substrates is based on reversible hydrolysis and condensation processes and described by various authors like Osterholtz and Pohl (1992), Altmann and Pfeiffer (2003), Chauhan, et al. (2008), Da Silva, Öchsner and Adams (2011, pp. 239–243), Kim, Holinga and Somorjai (2011), Yadav, et al. (2014), Deetz and Faller (2015) and Koç, Sert Çok and Gizli (2020); the influencing parameters are listed by Issa and Luyt (2019). The aim is to attach the condensation process resulting siloxane bonds covalently to the silanol groups (Si-OH) of the SiO₂ surface or neighbour molecules via hydrogen bonding or electrostatic interactions to a polysiloxane network. There are different ways for APTES to build several surface and layer structures like covalent attachment, horizontal polymerization through adjacent APTES molecules and multilayers resulting from the trifunctionality of APTES molecule, which leads to vertical polymerization described by Fadeev and McCarthy (1999), Asenath Smith and Chen (2008), Pasternack, Rivillon Amy and Chabal (2008), Acres, et al. (2012) and Yadav, et al. (2014). The investigated adhesion forces of ultraviolet (UV) polymer films with fixed weight or concentration of APTES and other organosilanes in the ink formulation or adhesion forces of UV polymer films on APTES- and other organosilane-functionalized glass substrates were investigated by Zhang, et al. (2013) and Wang, et al. (2021). Especially the investigations of Wang showed off the different wetting behaviour of functionalized glass surface based on the chemical diversity of the used silanes. Additionally, the wetting behaviour of APTES-functionalized glass surfaces depends on the applied functionalization method. The two widely used deposition methods are the solution-based method and the vapour-based method described by Metwalli, et al. (2006) and Liang, et al. (2014). The most commonly applied solutions for functionalization are ethanol/water solutions (95:5), recommended by Arkles, et al. (2014) or toluene solutions described by Arslan, et al. (2006), Fiorilli, et al. (2008), Pasternack, Rivillon Amy and Chabal (2008), Kim, Holinga and Somorjai (2011), and with 0.2 % to 2.0 % volume fraction silane concentration described by Argekar, Kirley and Schaefer (2013), but mostly only applied for Si wafers or microscope slides. For the vapour-based method, homemade apparatus, (room temperature) chemical vapour deposition ((RT-) CVD) and molecular layer deposition (MLD) are used, described by Zhang, et al. (2010) and Canané (2019).

The APTES functionalization in the vapour phase is preferred because of the smaller and sparser particles (diameter $\Phi < 30$ nm) and more uniform monolayer on the Si wafer surface in comparison with the solution-based deposition method, which makes controlled polymerization difficult and shows low reproducibility and disordered layers on a substrate as described by

Van Der Voort and Vansant (1996), Fiorilli, et al. (2008), Liang, et al. (2014), and Munief, et al. (2018). Under “optimal” controlled conditions, the silanes assemble on the surface in a high-quality uniform self-assembled monolayer (SAM) mentioned by Silberzan, et al. (1991) and Van Der Voort and Vansant (1996). Nevertheless, the functionalization results depend also, e.g., on the used glass substrate and applied cleaning method, silane concentration, conditioning, storage, and hydration of the surface, duration of functionalization, and curing conditions (e.g., duration, temperature, cooling) and lead to difficult control of silane structures and layers described by Van Der Voort and Vansant (1996), Siqueira Petri, et al. (1999), Altmann and Pfeiffer (2003), Metwalli, et al. (2006), Matinlinna, Zhu, Lerum and Chen (2012), and Lung and Tsoi (2018). The diversity of existent investigations of functionalized surfaces under different applied cleaning- and functionalization methods and post-treatments complicates the comparison of functionalization results. Investigations in functionalized float glass surfaces could not be found. The float glass used in this research is a flat glass product manufactured by the typical Pilkington process described in Pilkington (1969) and has an atmosphere side, also called air side (AS), and a bath side, also called tin side (TS), which shows different surface properties, especially different surface wetting properties depending on applied cleaning method as investigated by Lazauskas and Grigaliūnas (2012). With the possibility of generating different wetting properties on hydrophilic leveled float glass surfaces with only one silane, further insights into the adhesion behaviour of e.g., UV-inks dependent on the different wetting properties are allowed. This work investigates the APTES functionalization of hydrophilic polar alkaline cleaned float glass surfaces in the vapour and solution phases with the help of static and dynamic contact angle measurements and evaluates surface energy. Additionally, a hydrophobic non-polar polyethylene (PE) foil surface was investigated. The polar and non-polar surfaces are clearly differentiable by the water contact angle, surface energy, contact angle hysteresis, and drop age and show off the suitability of dynamic contact angle (DCA) measurements for indicating adhesion forces on surfaces. The applied APTES functionalization methods lead to reproducible and different wetting properties of the air and tin sides of the float glass and lead to clear, differentiable contact angle hysteresis and drop age when taking the glass side and the test fluid used into account. Appendix gives a summarized overview of measured static contact angles (SCAs), corresponding surface energies (SEs) and DCA parameters drop age and hysteresis in Tables A1 to A5. The investigations show the suitability of DCA measurement for indicating adhesive forces resulting from the applied vapour- and solution-based functionalization processes with APTES, depending on the float glass sides.

2. Materials and methods

2.1 Materials

Table 1 lists all solid materials and fluids used in this research for sample preparation and measurement.

Table 1: Materials and fluids used

Substrates	<ul style="list-style-type: none"> • Float glass, clear, seamed edge, 126 mm × 50 mm × 2 mm • PE adhesion foil without adhesive, transparent, thickness D: 0.06 mm, IFOHA
Cleaning agents	<ul style="list-style-type: none"> • Laboratory dishwasher cleaner, Neodisher Labo GK, Dr. Weigert • Ethanol, ≥ 99.8 %, denatured, CAS-no.: 64-17-5 • Water, Aqua Dest., CAS-no.: 7732-18-5, Wittig Umweltchemie
Functionalization agents	<ul style="list-style-type: none"> • 3-aminopropyltriethoxysilane, 98.0 %, CAS-no.: 919-30-2, Thermo Scientific™ • Acetic acid, 100.0 %, Ph. Eur., pure, CAS-no.: 64-19-7 • Ethanol, ≥ 99.8 %, denatured, CAS-no.: 64-17-5 • Double-distilled water, Aqua Bidest • Silica gel orange, size 2–5 mm, CAS-no.: 1327-36-2, Carl Roth
Static contact angle and dynamic contact angle test-liquids	<ul style="list-style-type: none"> • Water, Aqua Dest., Wittig Umweltchemie • Diiodomethane, 99.0 %, stab., CAS-no.: 75-11-6, Alfa Aesar • Benzyl alcohol, 99.0 %, CAS-no.: 100-51-6, Alfa Aesar • Glycerol, 99.0 %, CAS-no.: 56-81-5, Alfa Aesar

2.2 Cleaning method

The float glass used was cleaned in a 60 °C mildly alkaline cleaning bath (4 g/l laboratory dishwasher cleaner (LDC), pH: 11.3–11.4) in distilled water in a stainless steel container (353 mm × 325 mm × 65 mm) with a matching lid for 1 h on a hot plate (\approx 40 °C) followed by distilled water rinsing of the float glass samples in a mini-dishwashing machine (MD 37004, Medion) using program P2 (wash: 50 °C, rinse: 65 °C, dry: 1h) to remove coarse organic and inorganic contaminants, to get the float glass surfaces hydrophilic with water

contact angles (WCAs \approx 1° after 10 s) and to provide a basis for comparing the wetting behaviour of APTES-functionalized float glass surfaces. The used cleaning method is called the “enhanced cleaning method”, abbreviated EM. The cleaned float glass was stored for one week at room temperature in dust-free sample boxes before starting with the functionalization process.

2.3 Functionalization methodologies

The wetting behaviour of the cleaned float glass surfaces was changed by using two functionalization methods. The APTES functionalization was carried out via the vapour phase (M1) and via the solution phase (M2) in the style of Wang, et al. (2021) with different variants like duration of functionalization and silane concentration.

2.3.1 APTES functionalization via vapour phase

For the APTES functionalization in the vapour phase, the APTES listed in Table 1 was used. One to two days before APTES functionalization, the silica gel was activated in the drying oven for 2 h at 120 °C, cooled down, and stored in a little glass container. On functionalization day, 130 g of the activated silica gel was filled in the crystallizer bowl (outer diameter Φ_o : 80 mm, height H : 45 mm, volume V : 150 ml) and placed on the bottom of the desiccator (DN200, Duran). Afterwards, the APTES is pipetted into the eight silane reservoirs (V : 60 μ l each, Φ_o : 10 mm, inner diameter Φ_i : 6 mm, H : 6.7 mm) of the polytetrafluoroethylene (PTFE) functionalization ring (Φ_o : 115 mm, Φ_i : 90 mm, H : 5 mm) and placed around the crystallizer bowl with the silica gel in it.

The porcelain perforated plate was positioned in the desiccator, and two sample holders (polyoxymethylene) with 16 float glass samples were placed on the perforated plate. Near them, the thermo-hygrometer (TP157-3, ThermoPro) was placed and the desiccator was closed. Afterwards, the desiccator was placed onto the hot plate (40 °C) of the magnetic stirrer (RSM 10HS, Phoenix Instruments), and the vacuum pump (AS29, Wiltec) was connected to the desiccator tap. By starting the vacuum pump the valve of the desiccator tap had to be open. The vacuum pump was running for about 2 min, and resulting in an under pressure of 0.08 MPa inside the desiccator. After 2 min, the valve of the desiccator tap was closed, and the vacuum pump could be stopped. The vacuum procedure was repeated every hour because of the short vacuum holding of the desiccator (< 60 min). During the functionalization process, the inside temperature increased to 21.5 °C and relative humidity decreased to 16 %. After functionalization (duration: 2 h, 4 h and 8 h), each of the float

glass samples was cleaned with a cleanroom cloth surrounded plastic squeegee with ≈ 3 ml of ethanol three times with two repetitions. Afterwards, the functionalized batch was rinsed clean in the mini-dishwashing machine and conditioned at room temperature for three days in dust-free sample boxes. Within four days, the SCA and DCA measurements were carried out.

2.3.2 APTES functionalization via solution phase

For APTES functionalization in the solution phase, all the listed functionalization agents were used (Table 1). The APTES solution consists of a mass fraction of 95 % ethanol ($570 \text{ g} \pm 1 \text{ g}$) and a 5 % mass fraction of double-distilled water ($30 \text{ g} \pm 0.1 \text{ g}$) to reach a volume of ≈ 800 ml. Thereby, the double-distilled water was added drop by drop to the ethanol with the disposable pipette (V : 30 ml) and was mixed using the PTFE magnetic stirring rod ($L \times \Phi$: 35 mm \times 9 mm) in a laboratory bottle (V : 1000 ml) with closed screw cap for 20 min at 100 rounds per min (rpm); 5 min before the time was up, 12 g / 48 g of APTES (2 % / 8 % mass fraction of the ethanol/water solution) was weighed in. After weighing, the APTES was added drop by drop to the ethanol / water solution and mixed for another 20 min.

After the time was up, the APTES was pre-hydrolyzed and could be adjusted to a pH of 5.0 with acetic acid. The silane solution was decanted from the laboratory bottle into the crystallizer bowl (Φ_0 : 140 mm, H : 65 mm, V : 900 ml) with the magnetic stirring rod and was covered with a polyvinylidene fluoride (PVDF) plate with a small gap for the electrode of the pH-measurement device (HI98103, Hanna Instruments) held by a tripod. The electrode was dipped ≈ 10 mm in the silane solution and needed ≈ 2 min to show a constant pH. Acetic acid was added step by step with a disposable syringe (V : 10 ml) into the silane solution till a pH of 5.0 ± 0.1 was reached. All the time, the silane solution was mixed at 100 rpm.

Two hours after the end of mixing the APTES into the ethanol / water solution, the PVDF sample holder was placed in the silane solution-filled crystallizer bowl, followed by the placing of float glass samples in the sample holder with an acid-proof tweezers. The crystallizer bowl was covered by the PVDF plate, and the float glass functionalized for 1 h in the silane solution.

After functionalization, the cleaning procedure of Chapter 2.3.1 was carried out and afterwards the samples were stored in the drying oven (UN30 Plus, Memmert) for 1 h at 80 °C, and then finally clearly rinsed in the mini-dishwashing machine, and conditioned at room temperature in dust-free sample boxes for 3 days. Within four days, the SCA and DCA measurements were carried out.

2.4 Instruments

A contact angle measuring device (OCA 50, Dataphysics) was used to measure SCAs with the sessile drop method and DCAs with the sessile drop method and tilting plate with test fluids according to DIN EN ISO 19403-7 and DIN EN ISO 19403-6 (Deutsche Institut für Normung, 2020; 2023) to get quantitative data about the static and dynamic wetting behaviour of cleaned and APTES-functionalized float glass surfaces as well as the PE foil surface.

An AFM measurement device (Innova AFM, Bruker) was used to measure the R_q -roughness in two types of cleaned float glass surfaces. The float glass was first cleaned with the alkaline cleaning process described in Chapter 2.2 and in the following cleaning step, the alkaline cleaned float glass was cleaned in an acetone and ethanol ultrasonic cleaning bath for 5 min. After both cleaning procedures, the R_q -roughness was randomly evaluated of $10 \mu\text{m} \times 10 \mu\text{m}$ sections in tapping mode.

2.5 Static contact angle methodology

For the SCA measurement, the liquid drops of the test fluids water, diiodomethane, benzyl alcohol, and glycerol were used (Table 1). The adjusted contact angle measuring parameters and equipment used are listed in Table 2.

Table 2: Adjustments and equipment for static contact angle measurement using device OCA 50 of Dataphysics

Syringe	Disposable, V : 1 ml
Dosing needle	Φ_0 : 0.91 mm, Φ_1 : 0.58 mm, L : 38.1 mm
Dosing volume	2 μl
Dosing rate	0.10 $\mu\text{l/s}$
Method	Sessile drop
Brightness	Grey value between 170 and 200 in an area of ≈ 30 px over the positioned baseline; in the case of PE foil, adjustment to maximum.
Measurement table	Standard table for (functionalized) float glass, intake plate for planar fixing of PE foil
Live window size	1100 \times 730 px
Frame rate	22.39 frames per second
Contour fitting	Ellipse-fitting method

The liquid drops were placed with a disposable syringe and dosing needle on the EM-cleaned APTES-functionalized float glass surfaces and the PE foil surface. All measurements were done in a dark environment to avoid reflections in the liquid drop placed on the substrate surface. The dosed liquid drops were slowly picked up by the table used, and the applied liq-

uid drops lied for 10 s on the substrate surface to reach an approximate three-phase equilibrium. The application procedure was recorded by video and started by exceeding the optical trigger line that was placed near the drop curvature. The data fit of the first complete and sharply contoured lying drop on the surface, 3 frames after drop application, was used as the starting point for the evaluation of contact angle data over time. The mean contact angles (CAMs) were evaluated after frame 224 (approx. 10 s). For each test fluid, 20 CAMs on both glass sides and on the PE foil surface were carried out and evaluated. The following interpretations refer exclusively to the median of the SCA measurements.

2.6 Dynamic contact angle methodology

For the DCA measurement, the test liquids diiodomethane and water (Table 1), and adjustments and equipment given in Table 3 were used.

Table 3: Adjustments and equipment for dynamic contact angle measurement using device OCA 50 of Dataphysics

Syringe	Disposable, V: 1 ml
Dosing needle	Φ_0 : 1.83 mm, Φ_1 : 1.37 mm, L: 38.1 mm
Dosing volume	Diiodomethane: 4 μ l; water: 20 μ l
Dosing rate	0.10 μ l/s
Method	Sessile drop
Brightness	Grey value between 170 and 200 in an area of \approx 30 px over the positioned baseline; in the case of PE foil, adjustment to the maximum.
Measurement table	Standard table for (functionalized-) float glass, intake plate with membrane vacuum pump of Dataphysics for planar fixing of PE foil
Live window size	1600 px \times 730 px
Frame rate	10.00 frames per second
Electronic tilting device	Relative velocity of 0.5°/s (0.10°/step)
Contour fitting	Polynomial-fitting method

The test fluids were placed with a disposable syringe on the EM-cleaned APTES-functionalized float glass surfaces and the PE foil surface. The table was taped to the float glass sample format to create the best possible vacuum. The float glass sample was placed in the centre of the intake plate to arrange the camera and the sample in a T-shape position. The dosed liquid drop of each test liquid was slowly picked up with a standard table or the running intake plate after the drop dosing ended and lied for 10 s on the substrate surface. The video recording started shortly before picking up the dosed drop. After the drop was lying on the surface, a timer run up to 10 s and then the tilting was immediately manually started. The tilting was stopped manually when the liquid drop had rolled out of the live window. From the last tilting table data of 0.00°, the frames were counted up, and the corresponding advancing and receding contact angles were shown in diagrams of DCA measurements over frame time (100 frames \approx 10 s). On both float glass sides (cleaned and functionalized ones) and on the PE foil surface, 5 DCAs were captured with test fluids diiodomethane and water and evaluated.

3. Results of evaluated SCA measurements and SE

In the following sections, the measured SCAs on the float glass surfaces are evaluated and exemplarily shown in appropriate boxplot and table. The SCA results of the PE foil and the APTES-functionalized float glass surfaces (M1/M2) are displayed in tables. Additionally, the SEs of investigated surfaces are evaluated with the Owens, Wendt, Rabel, and Kaelble (OWRK) method (Owens and Wendt, 1969; Rabel, 1971; Kaelble, 1970).

3.1 The SCA results of EM-cleaned hydrophilic float glass surfaces

Evaluated SCAs of EM-cleaned float glass surfaces are listed in Table 4 and shown in Figure 1. The WCA results, evaluated at frame 35 (circle-fitted), of three

Table 4: Contact angles: median, min. and max. and deviation of 20 SCA measurements of the test fluids used on the AS and TS of the EM-cleaned float glass surfaces; an ellipse fitted WCA of \approx 1° after 10 s is assumed

SCA [°]	Water	Diiodomethane	Benzyl alcohol	Glycerol
AS	1.0	45.2	28.9	18.9
Min./Max.	–	44.1/46.7	27.0/29.6	17.6/20.3
Deviation	–	\pm 1.3	\pm 1.3	\pm 1.4
TS	1.0	42.1	22.1	20.8
Min./Max.	–	39.3/44.4	20.5/23.4	18.0/23.4
Deviation	–	\pm 2.6	\pm 1.5	\pm 2.7

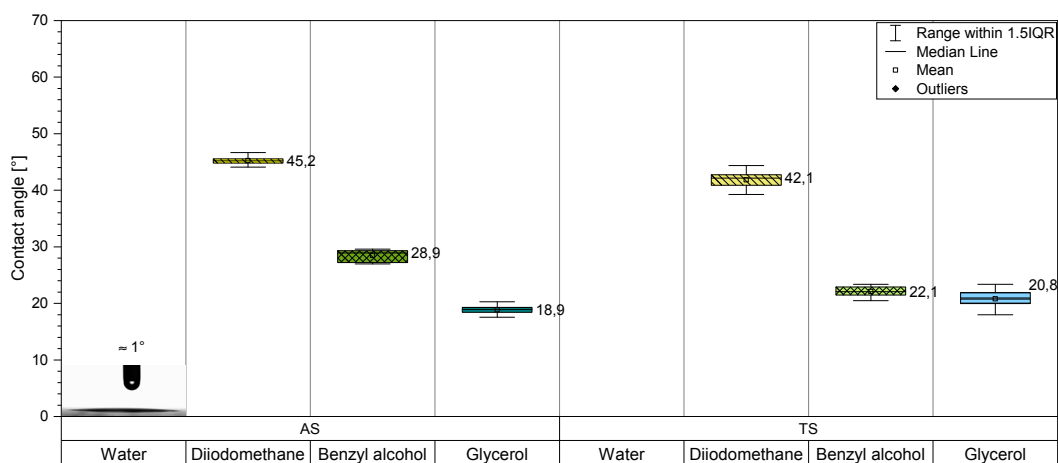


Figure 1: Solid contact angles of the EM-cleaned float glass surfaces with the test fluids used on the air side (AS) and the tin side (TS)

samples of EM-cleaned and one week at room temperature conditioned float glass were tested for normality with the Shapiro-Wilk test. One (GL_1) of the three samples showed normal distribution on both sides of the glass, with GL_1_1 DF (10), statistics: 0.927; $p = 0.423$ and GL_1_2, DF (10); statistics: 0.962; $p = 0.811$. This data series was tested for significance with the paired sample t -test and showed no significant difference between the glass sides (Table 5) and confirmed the result of Patejdl, Jung and Freieck (2022) with no significant difference between the wetting properties of the AS and TS after the alkaline cleaning procedure.

An ellipse-fitted WCA median of 1° was assumed after 10 s. The evaluated surface energies of the AS and TS complied with the leveling with SEs of 51.8 mJ/m^2 and 52.12 mJ/m^2 , respectively.

3.2 The SCA results of the hydrophobic PE foil surface

The SCA data of the PE foil surface (Table 6) show clearly the hydrophobic, non-polar wetting behaviour of the surface with a WCA median of 101.8° in comparison with the WCA data of hydrophilic EM-cleaned float glass surfaces (Table 6 vs Table 4). The SE of the PE foil surface was 30.9 mJ/m^2 , and much lower than the SEs of the EM-cleaned float glass surfaces, which were about 52.0 mJ/m^2 .

Further, the PE foil surface was more homogeneous, which can be seen in the deviations of CAM data in comparison with the EM-cleaned float glass surfaces (Table 6 vs Table 4). The PE foil surface is suitable as a benchmark for the homogeneity of surfaces.

Table 5: Significance tested by paired sample t -test on data series GL_1 AS to TS of the EM-cleaned float glass samples

Samples EM, DF(10)	t -statistic	Prob. > t	$p \leq .05$	$p \leq .01$	$p \leq .001$	Mean	SD	SEM	Median
GL_1_1	-2.106	0.064	-	-	-	5.128	0.987	0.312	5.366
GL_1_2			-	-	-	5.715	0.646	0.204	5.794

Table 6: Contact angles: median, min. and max. and deviation of SCA measurements of the test fluids used on the PE foil surface

SCA [°]	Water	Diiodomethane	Benzyl alcohol	Glycerol
PE foil	101.8	56.2	45.6	88.9
Min./Max.	100.6/102.3	55.6/57.0	44.5/46.0	86.9/89.7
Deviation	± 0.9	± 0.7	± 0.8	± 1.4



3.3 The SCA results of the M1 APTES-functionalized float glass surfaces in vapour phase

The EM-cleaned float glass was APTES-functionalized in the vapour phase by varying the functionalization duration (2 h, 4 h, 8 h). The comparison of the median WCA shows no increase in hydrophobicity with longer functionalisation times. Further, the WCA median of the AS and TS differed clearly in comparison to the EM-cleaned float glass surfaces. Exemplarily, these differences are shown in the Table 7 of the M1 (8 h) functionalized float glass surfaces. WCAs were evaluated on the AS between 35° and 41° and on the TS between 22° and 37° over functionalization durations of 2 h, 4 h and 8 h. The SEs were between 54.9 mJ/m² of M1 (2 h) and 55.2 mJ/m² of M1 (8 h) on the AS and on the TS between 55.6 mJ/m² of M1 (8 h) and 60.9 mJ/m² of M1 (2 h) and increased in comparison with the SEs of the EM-cleaned float glass surfaces.

3.4 SCA results of the M2 APTES-functionalized float glass surfaces in solution phase

The EM-cleaned float glass was APTES-functionalized in the solution phase with 2 % and 8 % silane concentrations in ethanol/water solution. The WCA median

of 2 % silane functionalized AS was 50° and on the TS 47.5° (Table 8). The WCA median of 8 % silane concentration showed despite of higher silane concentration, decreasing WCA median of 36.5° on the AS and 34.9° on the TS (Table 9). In contrast to APTES-functionalized float glass surfaces in vapour phase, the WCA median on the AS and TS of APTES-functionalized float glass surfaces in solution phase differed less. The SE on the AS of M2 (2 %) was 49.8 mJ/m² and on the TS 49.5 mJ/m². The SE on the AS of M2 (8 %) was 62.2 mJ/m² and on the TS 62.3 mJ/m².

4. Results of DCA measurement

The following subsections show exemplarily the DCA measurements and evaluated data (advancing and receding contact angle, drop age, baseline diameter (BD), tilt base (TB) and hysteresis) of investigated surfaces by using the test fluid diiodomethane. The DCA results of the test fluid water are included in chapter 4.5 and show their relevance only on the tin side of APTES-functionalized float glass surfaces. Appendix shows all evaluated SCAs, corresponding SEs and DCA parameters, hysteresis and drop age, for test fluids diiodomethane and water used (Tables A1 to A5).

Table 7: Contact angles: median, min. and max. and deviation of 20 SCA measurements of test fluids used on the AS and TS of the M1 (8 h) APTES-functionalized float glass surfaces

SCA [°]	Water	Diiodomethane	Benzyl alcohol	Glycerol
AS	37.8	37.5	14.9	39.3
Min./Max.	35.6/40.6	35.5/40.7	11.7/17.7	37.3/43.7
Deviation	± 2.5	± 2.6	± 3.0	± 3.2
				
TS	22.2	36.1	10.3	39.4
Min./Max.	18.7/31.9	34.0/37.4	9.7/13.2	36.5/42.7
Deviation	± 6.6	± 1.7	± 1.8	± 3.1
				

Table 8: Contact angles: median, min. and max. and deviation of 20 SCA measurements of the test fluids used on the AS and TS of the M2 (2 %) APTES-functionalized float glass surfaces

SCA [°]	Water	Diiodomethane	Benzyl alcohol	Glycerol
AS	50.3	40.7	11.5	44.0
Min./Max.	47.4/54.5	36.4/42.1	9.8/14.9	42.7/52.5
Deviation	± 3.6	± 2.9	± 2.6	± 4.9
				
TS	47.5	41.9	12.0	50.9
Min./Max.	43.5/52.8	39.8/43.5	7.5/16.8	46.4/53.9
Deviation	± 4.7	± 1.9	± 4.7	± 3.8
				

Table 9: Contact angles: median, min. and max. and deviation of 20 SCA measurements of the test fluids used on the AS and TS of the M2 (8 %) APTES-functionalized float glass surfaces

SCA [°]	Water	Diiodomethane	Benzyl alcohol	Glycerol
AS	36.5	31.5	2.0	33.9
Min./Max.	35.8/37.9	29.9/32.4	–	32.0/35.9
Deviation	± 1.1	± 1.3	–	± 2.0
				
TS	34.9	33.1	2.0	33.4
Min./Max.	31.6/38.5	32.2/34.0	–	30.9/36.6
Deviation	± 3.5	± 0.9	–	± 2.9
				

4.1 Results of DCA measurements on the EM-cleaned float glass surfaces

The DCA measurements on the EM-cleaned hydrophilic (polar) float glass surfaces with test fluid diiodomethane showed on the TS a higher hysteresis (39.8° to 42.0°) than on the AS (30.1° to 31.8°) (Figures 2, 3a; Table 10) and a longer drop age of the TS (72.9 s to 82.4 s) in comparison to the AS (59.9 s to 62.7 s) (Figure 3b; Table 10). The sharp drop part at the end of the advancing – and receding curves shows the incorrect polynomial fitting when the drop runs out of the measurement zone.

Out of the float glass manufacturing process, the TS (1–2 nm) is smoother than the AS (4–10 nm) as reported by Stiell (2002) and Silvestru, et al. (2018). The smoother surface results from the density differences between molten glass and tin. During the floating of molten glass on the tin bath, it is not unreasonable that the diffusing tin ions open the glass network by converting

bridging oxygens to non-bridging oxygens supported by the research of Šesták, Mareš and Hubík (2010) and Varshneya and Mauro (2019), just as network modifiers do. The alkaline cleaning bath used could attack the “weaker” TS more than the AS, which results in a higher surface roughness, an unsteady course of DCA measurements, and a larger hysteresis. This hypothesis can be supported by the research of Han, et al. (2016), which shows different Si wafer surface roughness after using different cleaning methods. AFM measurements showed on alkaline cleaned float glass surfaces the R_q roughness of 0.30 nm on the AS and 0.36 nm on the TS with relatively similar R_q roughness, but also assumed dust impurities, which complicate the evaluation of AFM measurements (Figure 4). An additional cleaning step with acetone and following ethanol ultrasonic bath led to better distinctions of roughness between AS and TS with 0.41 nm and 0.58 nm, respectively (Figure 5). The AFM results support the adoption of the “weaker” tin-side and the resulting larger hysteresis.

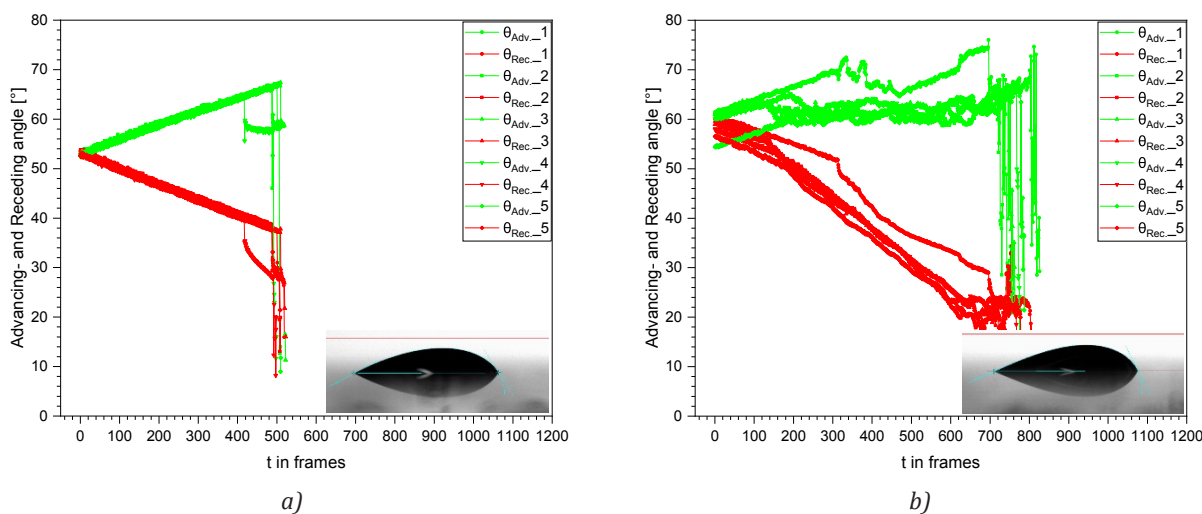


Figure 2: Dynamic contact angles on the EM-cleaned float glass surface, with the test fluid diiodomethane; air side (a), and tin side (b)

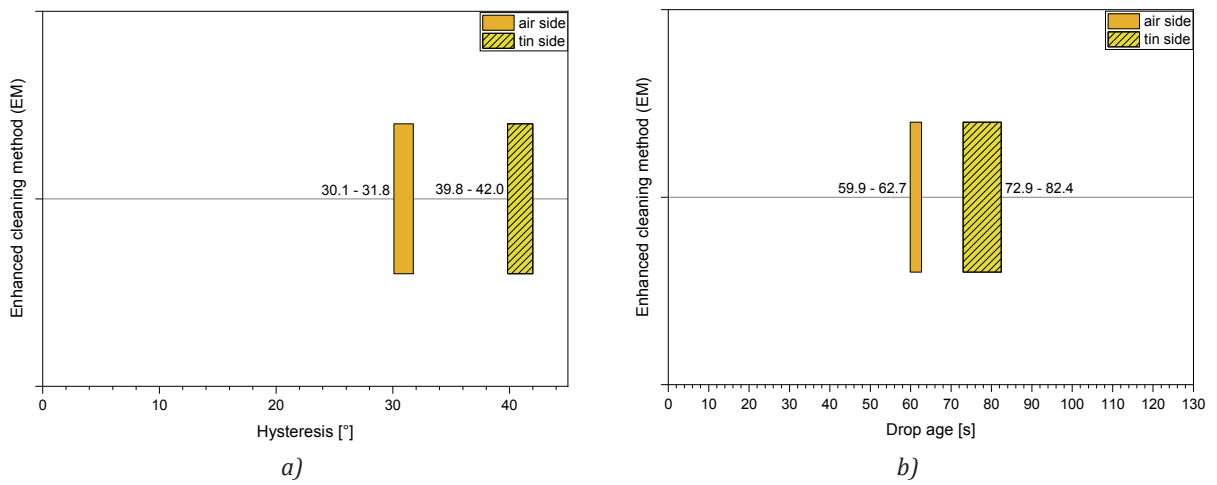


Figure 3: Diiodomethane drop (4 μ l) on the EM-cleaned float glass (AS/TS), hysteresis (a), and drop age (b)

Table 10: Evaluated DCA parameters of the EM-cleaned float glass surface with the test fluid diiodomethane

DCA glass		Adv. CA [°]	Rec. CA [°]	Drop age [s]	BD [mm]	TB [°]	Hysteresis [°]
AS	1	58.9	27.5	62.20	4.01	27.1	31.4
	2	58.7	28.4	61.29	3.95	26.2	30.3
	3	58.7	26.9	62.70	4.04	27.1	31.8
	4	58.1	27.9	59.90	4.01	25.6	30.1
	5	58.1	27.7	61.60	4.01	26.3	30.4
TS	1	64.9	22.9	82.40	3.96	37.4	41.9
	2	59.9	19.8	72.99	4.33	32.7	40.1
	3	62.3	22.4	74.80	4.06	33.4	39.8
	4	63.5	22.9	76.00	4.01	33.8	40.6
	5	61.9	20.4	73.80	4.16	32.7	41.5

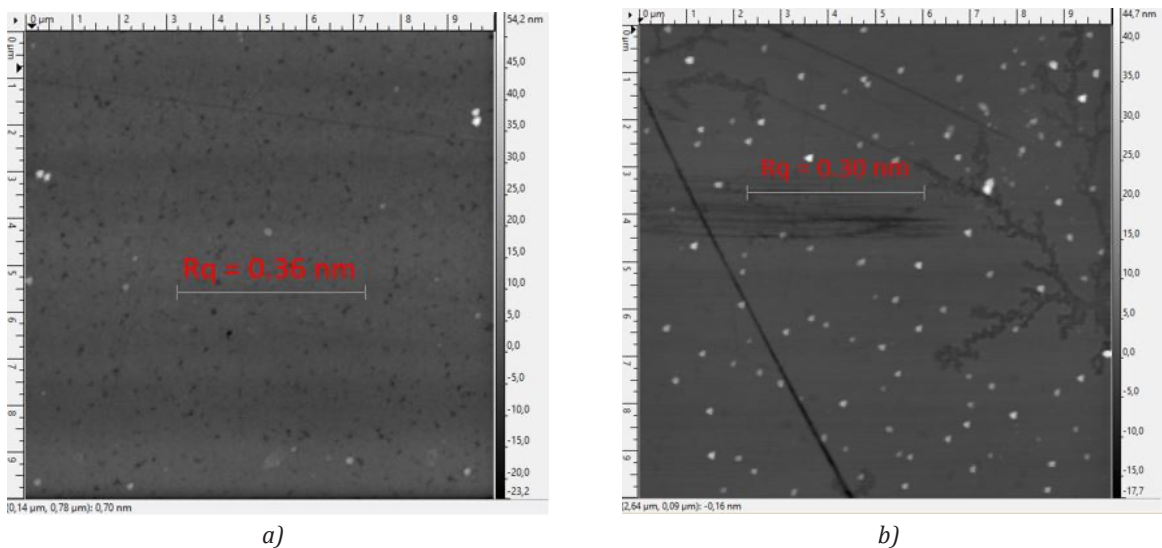


Figure 4: Atomic force microscopic measurement on the air and tin side after alkaline cleaning process with R_q roughness on the air side of 0.36 nm (a), and on the tin side 0.30 nm (b)

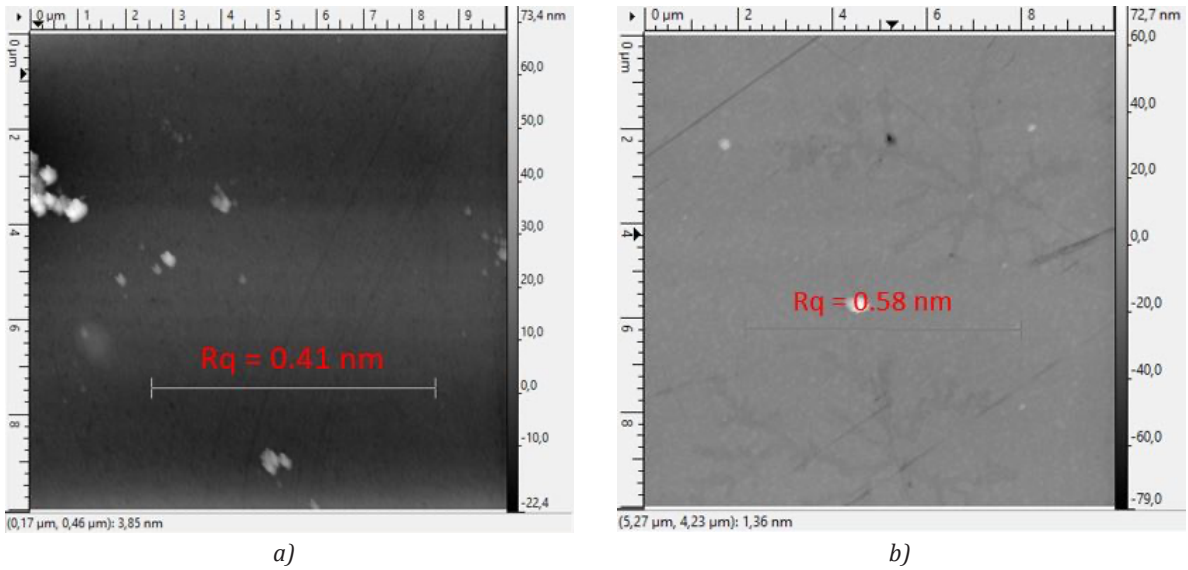


Figure 5: Atomic force microscopic measurement after alkaline cleaning process and afterwards following acetone and ethanol ultrasonic bath with R_q roughness on the air side of 0.41 nm (a), and on the tin side 0.58 nm (b)

The evaluated SEs of the AS (51.8 mJ/m²) and the TS (52.1 mJ/m²) seem to be first not sensitive to different surface properties of the EM-cleaned surfaces in comparison to the results of the DCA measurements.

4.2 Results of DCA measurements on the PE foil surface

The DCA measurements on the non-polar PE foil surface (WCA median: 101.8°) show, in contrast to the EM-cleaned float glass surfaces with assumed similar roughness, a low hysteresis (9.8° to 13.0°) (Figures 6, 7a; Table 11).

The unsteady course of DCA measurements at the end is caused by the unsteady position of the baseline during the contour fitting process.

The evaluation of the diiodomethane drop age on the PE foil surface is 28.9 s to 33.8 s (Figure 7b; Table 11), which is much shorter than on the EM-cleaned float glass surfaces. The DCA results of the hydrophilic float

glass surfaces and the hydrophobic PE foil surface confirm the suitability of using the DCA parameters hysteresis and drop age for indicating adhesion forces on functionalized float glass surfaces.

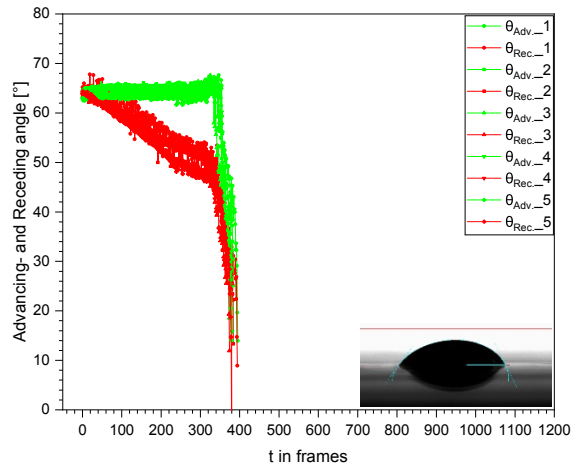
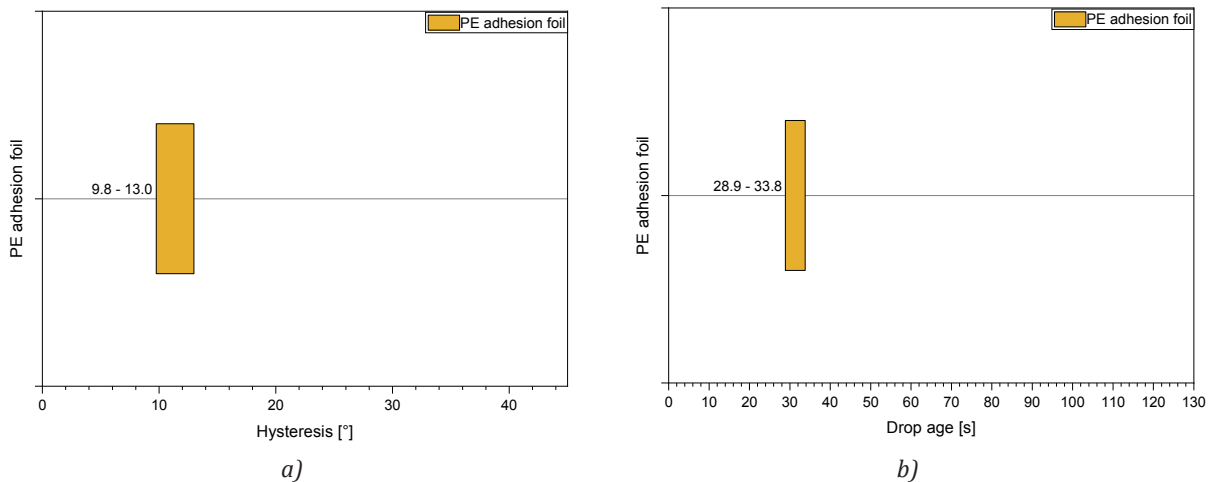


Figure 6: Dynamic contact angles on the PE foil surface with the test fluid diiodomethane

Table 11: Evaluated DCA parameters of the PE foil surface with the test fluid diiodomethane

DCA PE foil	Adv. CA [°]	Rec. CA [°]	Drop age [s]	BD [mm]	TB [°]	Hysteresis [°]
1	65.0	54.9	33.79	3.43	11.8	10.1
2	65.6	52.6	31.69	3.44	10.5	12.9
3	64.7	54.9	29.59	3.50	9.8	9.8
4	63.9	53.8	28.89	3.74	9.3	10.1
5	63.3	51.5	30.99	3.50	10.8	11.8



a) *Figure 7: Diiodomethane drop (4 μ l) on the PE foil surface, hysteresis (a), and drop age (b)*

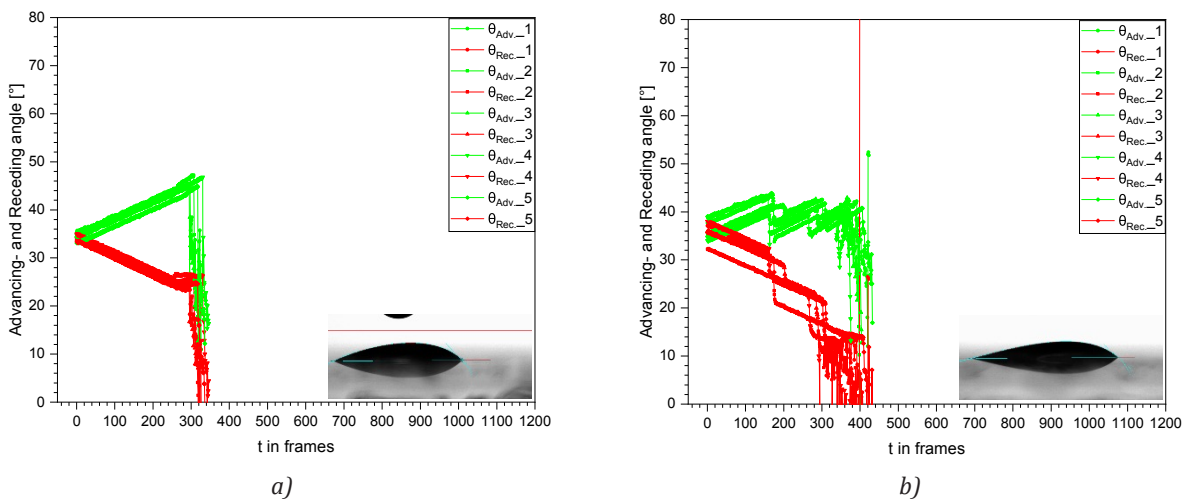
4.3 Results of DCA measurements of the M1 APTES-functionalized float glass surfaces in vapour phase

The DCA measurements and evaluated parameters of M1 APTES-functionalized float glass surfaces in the vapour phase are exemplarily shown for the test fluid diiodomethane and M1 (8 h) (Figure 8; Table 12). By ordering the evaluated DCA parameters, hysteresis and drop age, to increasing WCA medians, and differentiating between the AS and TS and the test fluids diiodomethane and water, of the investigated EM-cleaned float glass surfaces, M1 APTES-functionalized float glass surfaces, and the PE foil surface, partial inconsistencies in hysteresis and drop age are visible (Figure 9). A plausible explanation is incomplete functionalization, which leads to inhomogeneous surface properties. Despite these inconsistencies, the comparison of the polar

and non-polar surfaces is acceptable. For the further course, only the M1 (8 h) functionalization was taken into account for the final evaluations in section 4.5. Here, a completely functional surface can be expected.

4.4 Results of DCA measurements of the M2 APTES-functionalized float glass surfaces in solution phase

The DCA measurements and evaluated parameters of M2 APTES-functionalized float glass surfaces in the solution phase are exemplarily shown for the test fluid diiodomethane (Figures 10 to 12; Tables 13, 14). By ordering the evaluated DCA parameters, hysteresis and drop age, to increase WCA and differentiating between the AS and TS and the test fluids diiodomethane and water, of the investigated EM-cleaned float glass, M2 APTES-functionalized float glass, and the PE foil sur-



a) *Figure 8: Dynamic contact angles on M1 (8 h) APTES-functionalized float glass surface with the test fluid diiodomethane, air side (a), and tin side (b)*

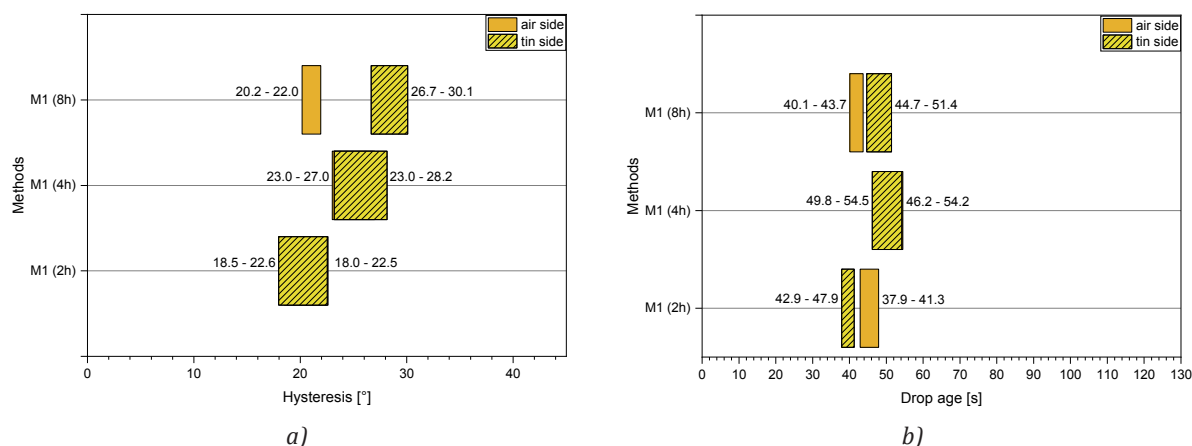


Figure 9: Diiodomethane drop (4 µl) on the M1 APTES-functionalized float glass surfaces in vapour phase (AS/TS), hysteresis (a), and drop age (b)

Table 12: Evaluated DCA parameters of the M1 (8 h) APTES-functionalized float glass surfaces with the test fluid diiodomethane

DCA glass	Adv. CA [°]	Rec. CA [°]	Drop age [s]	BD [mm]	TB [°]	Hysteresis [°]	
AS	1	44.7	23.3	40.09	4.10	15.4	21.4
	2	47.1	25.2	41.60	4.10	15.8	21.9
	3	45.1	24.1	40.60	4.18	15.2	20.9
	4	46.8	26.3	43.70	4.00	17.2	20.6
	5	44.7	24.6	42.39	4.09	16.4	20.2
TS	1	41.9	13.2	49.90	5.00	20.3	28.7
	2	41.4	11.3	46.09	5.00	18.3	30.1
	3	42.1	13.9	48.70	4.77	19.3	28.2
	4	39.5	12.7	44.70	5.19	17.7	26.8
	5	40.7	14.1	51.39	4.71	21.2	26.7

face, the data show consistency and are plausible in comparison of the polar and non-polar surfaces, too. For the M2 (2 %) and M2 (8 %) variants of solution

phase functionalization are taken into account for the final evaluations. A completely functional surface can be expected.

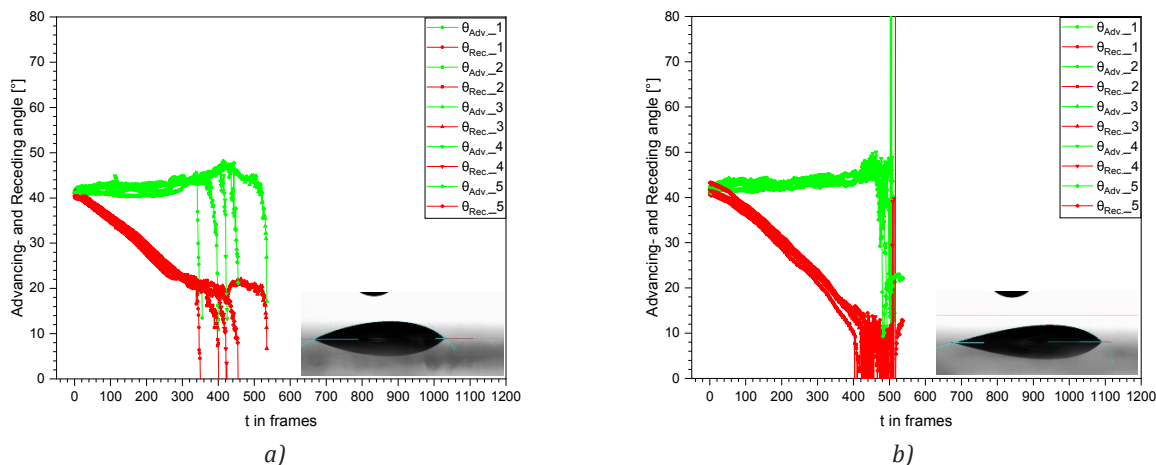


Figure 10: Dynamic contact angles on the M2 (2 %) APTES-functionalized float glass surface with the test fluid diiodomethane, air side (a), and tin side (b)

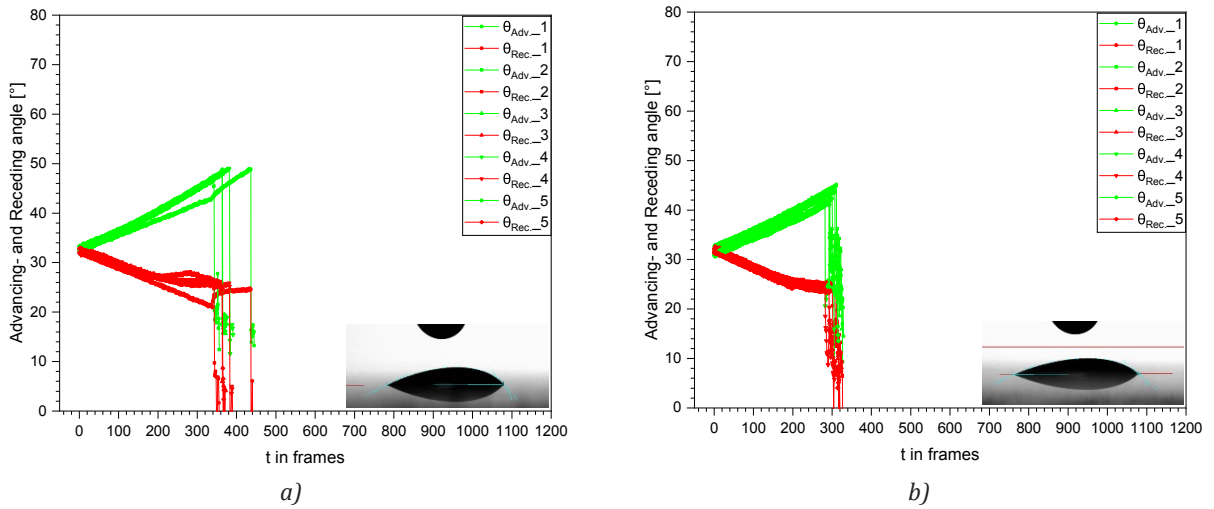


Figure 11: Dynamic contact angles on the M2 (8%) APTES-functionalized float glass surface with the test fluid diiodomethane, air side (a), and tin side (b)

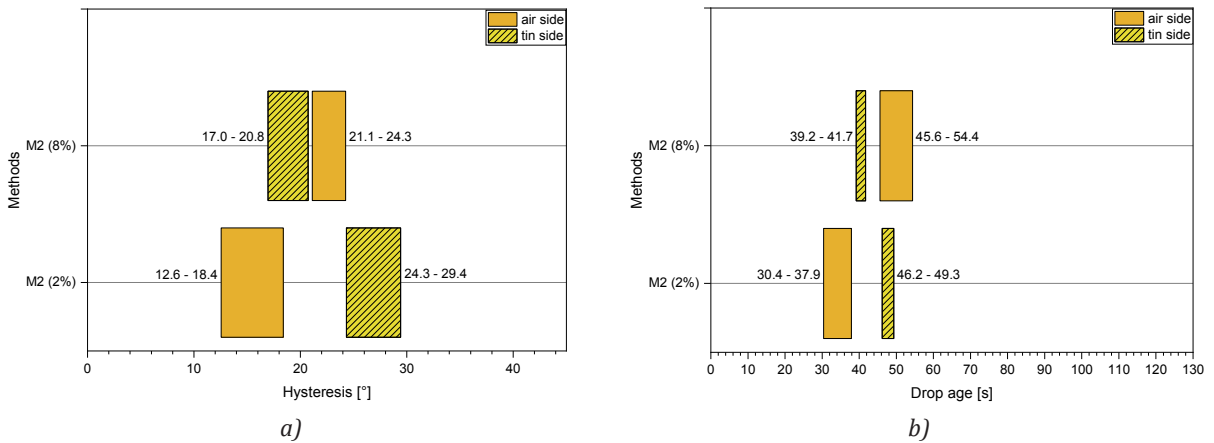


Figure 12: Diiodomethane drop (4 μl) on the M2 (8%) APTES-functionalized float glass surfaces (AS/TS), hysteresis (a), and drop age (b)

Table 13: Evaluated dynamic contact angle parameters of the M2 (2%) APTES-functionalized float glass surfaces with the test fluid diiodomethane

DCA glass		Adv. CA [°]	Rec. CA [°]	Drop age [s]	BD [mm]	TB [°]	Hysteresis [°]
AS	1	41.7	27.1	30.99	4.40	10.6	14.6
	2	40.6	27.9	30.40	4.24	10.2	12.6
	3	42.8	25.2	37.90	4.30	13.8	17.6
	4	43.2	24.8	36.80	4.45	13.4	18.4
	5	43.0	25.6	36.79	4.25	13.3	17.4
TS	1	44.9	15.5	49.30	4.68	19.9	29.4
	2	43.3	14.2	47.60	4.93	18.9	29.1
	3	42.3	18.2	46.19	4.60	18.0	26.1
	4	42.9	18.6	46.20	4.65	18.1	24.3
	5	45.1	15.9	48.30	4.84	19.4	29.1

Table 14: Evaluated dynamic contact angle parameters of the M2 (8 %) APTES-functionalized float glass surfaces with the test fluid diiodomethane

DCA glass		Adv. CA [°]	Rec. CA [°]	Drop age [s]	BD [mm]	TB [°]	Hysteresis [°]
AS	1	48.9	24.6	54.39	3.66	22.8	24.3
	2	46.6	25.5	45.60	3.90	17.9	21.1
	3	47.8	25.9	47.19	3.91	18.7	21.9
	4	48.7	25.8	48.89	3.80	19.9	22.9
	5	48.3	24.8	47.19	3.90	18.8	23.5
TS	1	45.0	24.3	41.50	4.07	16.2	20.7
	2	42.4	25.4	40.69	3.92	15.6	16.9
	3	43.9	23.7	41.70	4.14	15.9	20.3
	4	43.2	25.2	39.19	4.12	14.8	17.9
	5	41.8	23.3	40.50	4.07	15.2	18.5

4.5 Results of DCA measurements under assumed complete functionalization of float glass surfaces

Tables 15 and 16 show the evaluated hysteresis and drop age ranges of M1 (8 h), M2 (2 %) and M2 (8 %) APTES-functionalized float glass surfaces. These variants are assumed to be completely functionalized and are plau-

sible in comparison with the polar and non-polar surfaces by ordering the DCA parameters with an increase of WCA median considering difference between the AS and TS and the test fluids diiodomethane and water.

The results show consistency by using the test fluid diiodomethane on the AS and the test fluid water on the TS.

Table 15: Comparison of assumed saturated APTES functionalization methods ordered after hydrophobization grade with the test fluid diiodomethane (AS)

	Polar surface	Dynamic contact angle measurements Hydrophobic direction →			Non-polar surface
		M2 (8 %)	M1 (8 h)	M2 (2 %)	
Material/ Methods	EM-cleaned DCA: ~1.0° SE: 51.83 mJ/m ²	M2 (8 %) DCA: 36.5° SE: 62.10 mJ/m ²	M1 (8 h) DCA: 37.8° SE: 55.20 mJ/m ²	M2 (2 %) DCA: 50.3° SE: 49.80 mJ/m ²	PE DCA: 101.8° SE: 45.35 mJ/m ²
Parameter					
Hysteresis [°]	30.1–31.8	21.1–24.3	20.2–21.9	12.6–18.4	9.8–12.9
Drop age [s]	59.90–62.70	45.60–54.39	40.09–43.70	30.40–37.90	28.89–33.79

Table 16: Comparison of assumed saturated APTES functionalization methods ordered after hydrophobization grade with the test fluid water (TS)

	Polar surface	Dynamic contact angle measurements Hydrophobic direction →			Non-polar surface
		M1 (8 h)	M2 (8 %)	M2 (2 %)	
Material/ Methods	EM-cleaned WCA: ~1.0° SE: 52.12 mJ/m ²	M1 (8 h) WCA: 22.2° SE: 59.90 mJ/m ²	M2 (8 %) WCA: 34.9° SE: 62.30 mJ/m ²	M2 (2 %) WCA: 47.5° SE: 49.50 mJ/m ²	PE WCA: 101.8° SE: 45.35 mJ/m ²
Parameter					
Hysteresis [°]	< 10	21.6–30.1	27.0–32.8	39.2–43.2	< 10
Drop age [s]	-	63.19–77.69	75.49–85.69	114.89–130.39	-

5. Conclusion

The dynamic contact angle measurement can be used as an indicator for adhesion forces on different APTES-functionalized float glass surfaces with different wetting properties.

The EM-cleaned hydrophilic polar float glass surfaces (WCA median: $\approx 1^\circ$) showed on the tin side a higher hysteresis between 39.8° and 42.0° than on the air side with a hysteresis between 30.1° and 31.8° of diiodomethane drop. The tin side also showed a higher drop age between 72.9 s and 82.4 s than the air side with a drop age between 59.9 s and 62.7 s. Despite very similar surface energies of 51.8 mJ/m^2 and 52.1 mJ/m^2 , the hysteresis and the drop age are parameters that showed clear tendencies for the EM-cleaned float glass surfaces. Both parameters indicated an increase in adhesion forces on the tin side of the float glass. AFM measurements showed a higher surface roughness on the tin side in comparison with the air side after the additional cleaning step with acetone and ethanol ultrasonic cleaning bath and explain the higher hysteresis and drop age on the tin side.

In contrast, the hydrophobic non-polar smooth PE foil surface (WCA median: 101.8°) showed a small hysteresis between 9.7° and 12.9° with a short drop age between 28.8 s and 33.7 s of diiodomethane drop in correlation with a low surface energy of 30.9 mJ/m^2 .

The DCA results of the hydrophilic float glass surfaces and the hydrophobic PE foil surface confirmed the suitability of using the DCA parameters hysteresis and drop age for indicating adhesion forces on functionalized float glass surfaces.

The float glass surfaces APTES-functionalized in the vapour phase were investigated with static and dynamic contact angle measurements with test fluids diiodomethane and water. The vapour-functionalized float glass surfaces clearly showed the two-sidedness of float glass. On the air side, the WCA median was between 35.7° and 41.1° and on the tin side, the WCA median was between 22.2° and 37.1° . These results

show the slower functionalization of tin side in comparison with the air side by using the vapour-phase method. The varying functionalization duration does not lead to a stronger hydrophobic wetting effect on the surfaces. The measurements of homogeneous functionalized float glass surfaces (preparation time of 8 h) showed a clear hysteresis and drop age difference between the air and tin side with the test fluid diiodomethane.

The float glass surfaces APTES-functionalized in the solution phase showed off clearly differentiable water contact angles dependent on the silane concentration. In contrast to the functionalization in the vapour phase the WCA medians of the air and tin sides differed not so much from each other. By evaluating the 2 % concentration, the static contact angle measurements showed an air side WCA median of 50.3° and a tin side WCA median of 47.5° . By evaluating the 8 % concentration, the static angle measurements showed on the air side a WCA median of 36.5° and on the tin side a WCA median of 34.9° .

The results of WCA median, surface energy, hysteresis, and drop age of EM-cleaned, vapour-phase functionalized (8 h), and solution-phase functionalized (2 % and 8 %) float glass surfaces, and the PE foil surface were shown in order of increasing water contact angle, separately for the air and tin sides, and test fluids diiodomethane and water. The application of the test fluid diiodomethane on the air side and the test fluid water on the tin side of functionalized float glass surfaces confirmed the prediction that an increased water contact angle leads to a clear decrease or increase of hysteresis and drop age. This confirmed again the suitability of using the DCA parameters hysteresis and drop age for indicating adhesion forces on functionalized float glass surfaces. Disperse and polar components of functionalized surfaces are not suitable for analysis of adhesion forces on APTES-functionalized float glass surfaces.

With this research a better understanding of e.g., UV-ink adhesion forces dependent on glass surface wetting properties could be reached.

References

- Acres, R.G., Ellis, A.V., Alvino, J., Lenahan, C.E., Khodakov, D.A., Metha, G.F. and Andersson, G.G., 2012. Molecular structure of 3-aminopropyltriethoxysilane layers formed on silanol-terminated silicon surfaces. *The Journal of Physical Chemistry C*, 116(10), pp. 6289–6297. <https://doi.org/10.1021/jp212056s>.
- Altmann, S. and Pfeiffer, J., 2003. The hydrolysis/condensation behaviour of methacryloyloxyalkylfunctional alkoxysilanes: structure-reactivity relations. *Monatshefte für Chemie / Chemical Monthly*, 134(8), pp. 1081–1092. <https://doi.org/10.1007/s00706-003-0615-y>.
- Argekar, S.U., Kirley, T.L. and Schaefer, D.W., 2013. Determination of structure-property relationships for 3-aminopropyltriethoxysilane films using x-ray reflectivity. *Journal of Material Research*, 28(8), pp. 1118–1128. <https://doi.org/10.1557/jmr.2013.54>.

- Arkles, B., Maddox, A., Singh, M., Zzyczny, J. and Matisons, J., 2014. *Silane coupling agents: connecting across boundaries*. 3rd ed. Morrisville, PA, USA: Gelest.
- Arslan, G., Ozmen, M., Gündüz, B., Zhang, X. and Ersöz, M., 2006. Surface modification of glass beads with an aminosilane monolayer. *Turkish Journal of Chemistry*, 30(2), pp. 203–210.
- Asenath Smith, E. and Chen, W., 2008. How to prevent the loss of surface functionality derived from aminosilanes. *Langmuir*, 24(21), pp. 12405–12409. <https://doi.org/10.1021/la802234x>.
- Canané, P., 2019. *Silanization by room temperature chemical vapor deposition and controlled roughness for wettability modification of microfabrication substrates*. [pdf] Available at: < <https://fenix.tecnico.ulisboa.pt/downloadFile/844820067126289/SilanizationbyRoomTemperatureChemicalVaporDepositionandControlledRoughnessforWettabilityModificationofMicro.pdf> > [Accessed August 2023].
- Chauhan, A.K., Aswal, D.K., Koiry, S.P., Gupta, S.K., Yakhmi, J.V., Sürgers, C., Guerin, D., Lenfant, S. and Vuillaume, D., 2008. Self-assembly of the 3-aminopropyltrimethoxysilane multilayers on Si and hysteretic current–voltage characteristics. *Applied Physics A*, 90(3), pp. 581–589., <https://doi.org/10.1007/s00339-007-4336-7>.
- Da Silva, L.F.M., Öchsner, A. and Adams, R.D. eds., 2011. *Handbook of adhesion technology*. Cham: Springer.
- Deetz, J.D. and Faller, R., 2015. Reactive modeling of the initial stages of alkoxy silane polycondensation: effects of precursor molecule structure and solution composition. *Soft Matter*, 11(34), pp. 6780–6789. <https://doi.org/10.1039/C5SM00964B>.
- Deutsche Institut für Normung, 2020. *DIN EN ISO 19403-7:2020-04 Paints and varnishes – Wettability – Part 7: Measurement of the contact angle on a tilt stage (roll-off angle)*. Berlin: DIN, Beuth Verlag.
- Deutsche Institut für Normung, 2023. *DIN EN ISO 19403-6:2023-10 Draft Paints and varnishes – Wettability – Part 6: Measurement of dynamic contact angle*. Berlin: DIN, Beuth Verlag.
- Fadeev, A.Y. and McCarthy, T.J., 1999. Trialkylsilane monolayers covalently attached to silicon surfaces: wettability studies indicating that molecular topography contributes to contact angle hysteresis. *Langmuir*, 15(11), pp. 3759–3766. <https://doi.org/10.1021/la981486o>.
- Fiorilli, S., Rivolo, P., Descrovi, E., Ricciardi, C., Pasquardini, L., Lunelli, L., Vanzetti, L., Pederzoli, C., Onida, B. and Garrone, E., 2008. Vapor-phase self-assembled monolayers of aminosilane on plasma-activated silicon substrates. *Journal of Colloid and Interface Science*, 321(1), pp. 235–241. <https://doi.org/10.1016/j.jcis.2007.12.041>.
- Han, Y., Mayer, D., Offenhäusser, A. and Ingebrandt, S., 2006. Surface activation of thin silicon oxides by wet cleaning and silanization. *Thin Solid Films*, 510(1–2), pp. 175–180. <https://doi.org/10.1016/j.tsf.2005.11.048>.
- Issa, A.A. and Luyt, A.S., 2019. Kinetics of alkoxy silanes and organoalkoxy silanes polymerization: a review. *Polymers*, 11(3): 537. <https://doi.org/10.3390/polym11030537>.
- Kaelble, D.H., 1970. Dispersion-polar surface tension properties of organic solids. *The Journal of Adhesion*, 2(2), pp. 66–81. <https://doi.org/10.1080/0021846708544582>.
- Kim, J., Holinga, G.J. and Somorjai, G.A., 2011. Curing induced structural reorganization and enhanced reactivity of amino-terminated organic thin films on solid substrates: observations of two types of chemically and structurally unique amino groups on the surface. *Langmuir*, 27(9), pp. 5171–5175. <https://doi.org/10.1021/la2007205>.
- Koç, F., Sert Çok, S. and Gizli, N., 2020. Tuning the properties of silica aerogels through pH controlled sol-gel processes. *Research on Engineering Structures and Materials*, 6(3), pp. 257–269. <http://dx.doi.org/10.17515/resm2019.166ma1203>.
- Lazauskas, A. and Grigaliūnas, V., 2012. Float glass surface preparation methods for improved chromium film adhesive bonding. *Materials Science / Medžiagotyra*, 18(2), pp. 181–186. <https://doi.org/10.5755/j01.ms.18.2.1924>.
- Liang, Y., Huang, J., Zang, P., Kim, J. and Hu, W., 2014. Molecular layer deposition of APTES on silicon nanowire biosensors: surface characterization, stability and pH response. *Applied Surface Science*, 322, pp. 202–208. <https://doi.org/10.1016/j.apsusc.2014.10.097>.
- Matinlinna, J.P., Lung, C.Y.K. and Tsoi, J.K.H., 2018. Silane adhesion mechanism in dental applications and surface treatments: a review. *Dental Materials*, 34(1), pp. 13–28. <https://doi.org/10.1016/j.dental.2017.09.002>.
- Metwalli, E., Haines, D., Becker, O., Conzone, S. and Pantano, C.G., 2006. Surface characterizations of mono-, di-, and tri-aminosilane treated glass substrates. *Journal of Colloid and Interface Science*, 298 (2), pp. 825–831. <https://doi.org/10.1016/j.jcis.2006.03.045>.
- Mittal, K.L. and O'kane, D.F., 1976. Vapor deposited silanes and other coupling agents. *The Journal of Adhesion*, 8(1), pp. 93–97. <https://doi.org/10.1080/00218467608075073>.
- Munief, W.-M., Heib, F., Hempel, F., Lu, X., Schwartz, M., Pachauri, V., Hempelmann, R., Schmitt, M. and Ingebrandt, S., 2018. Silane deposition via gas-phase evaporation and high-resolution surface characterization of the ultrathin siloxane coatings. *Langmuir*, 34(35), pp. 10217–10229. <https://doi.org/10.1021/acs.langmuir.8b01044>.
- Osterholtz, F.D. and Pohl, E.R., 1992. Kinetics of the hydrolysis and condensation of organofunctional alkoxy silanes: a review. *Journal of Adhesion Science and Technology*, 6(1), pp. 127–149. <https://doi.org/10.1163/156856192X00106>.
- Owens, D.K. and Wendt, R.C., 1969. Estimation of the surface free energy of polymers. *Journal of Applied Polymer Science*, 13(8), pp. 1741–1747. <https://doi.org/10.1002/app.1969.070130815>.

- Pasternack, R.M., Rivillon Amy, S. and Chabal, Y.J., 2008. Attachment of 3-(aminopropyl)triethoxysilane on silicon oxide surfaces: dependence on solution temperature. *Langmuir*, 24(22), pp. 12963–12971. <https://doi.org/10.1021/la8024827>.
- Patejdl, S., Jung, U. and Freieck, K., 2022. Wetting and adhesion phenomena of surface-treated float glass. In: C. Ridgway, ed. *Advances in Printing and Media Technology: Proceedings of the 48th International Research Conference of iarigai*. Greenville, USA, 19–21 September 2022. Darmstadt: iarigai. https://doi.org/10.14622/Advances_48_2022_03.
- Pilkington, L.A.B., 1969. *Review lecture: the float glass process. Proceedings of the Royal Society of London A*, 314(1516), pp. 1–25. <https://doi.org/10.1098/rspa.1969.0212>.
- Plueddemann, E.P., 1970. Adhesion through silane coupling agents. *The Journal of Adhesion*, 2(3), pp. 184–201. <https://doi.org/10.1080/0021846708544592>.
- Plueddemann, E.P., 1991. *Silane coupling agents*. 2nd ed. Boston, MA, USA: Springer US.
- Rabel, W., 1971. Einige Aspekte der Benetzungstheorie und ihre Anwendung auf die Untersuchung und Veränderung der Oberflächeneigenschaften von Polymeren. *Farbe und Lack*, 77, pp. 997–1005.
- Silberzan, P., Leger, L., Ausserre, D. and Benattar, J.J., 1991. Silanation of silica surfaces. A new method of constructing pure or mixed monolayers. *Langmuir*, 7(8), pp. 1647–1651. <https://doi.org/10.1021/la00056a017>.
- Silvestru, V.A., Drass, M., Enghardt, O. and Schneider, J., 2018. Performance of a structural acrylic adhesive for linear glass-metal connections under shear and tensile loading. *International Journal of Adhesion and Adhesives*, 85, pp. 322–336. <https://doi.org/10.1016/j.ijadhadh.2018.07.006>.
- Siqueira Petri, D.F., Wenz, G., Schunk, P. and Schimmel, T., 1999. An improved method for the assembly of amino-terminated monolayers on SiO₂ and the vapor deposition of gold layers. *Langmuir*, 15(13), pp. 4520–4523. <https://doi.org/10.1021/la981379u>.
- Stiell, W., 2002. *Haftverhalten von Dichtstoffen auf beschichtetem und unbeschichtetem Glas*. Rosenheim: ift Rosenheim.
- Šesták, J., Mareš, J. and Hubík, P. eds., 2010. *Glassy, amorphous and nano-crystalline materials: thermal physics, analysis, structure and properties*. Dordrecht, New York: Springer.
- Van Der Voort, P. and Vansant, E.F., 1996. Silylation of the silica surface a review. *Journal of Liquid Chromatography & Related Technologies*, 19(17–18), pp. 2723–2752. <https://doi.org/10.1080/10826079608015107>.
- Varshneya, A.K. and Mauro, J.C., 2019. *Fundamentals of inorganic glasses*. 3rd ed. Amsterdam, Netherlands: Elsevier.
- Wang, Y., Hansen, C.J., Wu, C.-C., Robinette, E.J. and Peterson, A.M., 2021. Effect of surface wettability on the interfacial adhesion of a thermosetting elastomer on glass. *RSC Advances*, 11(49), pp. 31142–31151. <https://doi.org/10.1039/D1RA05916E>.
- Wolf, A.T., 2022. Organofunktionelle Silane als Haftvermittler. *Chemie in unserer Zeit*, 56(1), pp. 22–33. <https://doi.org/10.1002/ciuz.202000038>.
- Yadav, A.R., Sriram, R., Carter, J.A. and Miller, B.L., 2014. Comparative study of solution-phase and vapor-phase deposition of aminosilanes on silicon dioxide surfaces. *Materials Science and Engineering C*, 35, pp. 283–290. <https://doi.org/10.1016/j.msec.2013.11.017>.
- Zhang, F., Sautter, K., Larsen, A.M., Findley, D.A., Davis, R.C., Samha, H. and Linford, M.R., 2010. Chemical vapor deposition of three aminosilanes on silicon dioxide: surface characterization, stability, effects of silane concentration, and cyanine dye adsorption. *Langmuir*, 26(18), pp. 14648–14654. <https://doi.org/10.1021/la102447y>.
- Zhang, K., Li, T., Zhang, T., Wang, C. and Wu, M., 2013. Adhesion improvement of UV-curable ink using silane coupling agent onto glass substrate. *Journal of Adhesion Science and Technology*, 27(13), pp. 1499–1510. <https://doi.org/10.1080/01694243.2012.746159>.
- Zhu, M., Lerum, M.Z. and Chen, W., 2012. How to prepare reproducible, homogeneous, and hydrolytically stable aminosilane-derived layers on silica. *Langmuir*, 28(1), pp. 416–423. <https://doi.org/10.1021/la203638g>.

Appendix: Overview of static and dynamic- contact angle results of test fluids diiodomethane and water, and surface energies (Tables A1 to A5).

Table A1: SCA, SE (with disperse (γ^d_s), and polar (γ^p_s) components) and DCA results on the AS of float glass with the test fluid diiodomethane

Methods	Static contact angle measurements (2 μ l) [°]				Surface energy [mJ/m ²]	Dynamic contact angle measurements (diiodomethane)	
	Water	Diiodomethane	Benzyl alc.	Glycerol		Hysteresis [°]	Drop age [s]
EM	1.0	45.2	28.9	18.9	51.83 γ^d_s : 30.36 γ^p_s : 21.47	30.09–31.76	59.90–62.70
M1 (2 h)	41.1	35.3	14.7	36.6	54.92 γ^d_s : 30.78 γ^p_s : 24.14	18.50–22.62	42.90–47.90
M1 (4 h)	35.7	39.7	18.5	32.7	56.36 γ^d_s : 28.34 γ^p_s : 28.02	23.01–26.97	49.79–54.49
M1 (8 h)	37.8	37.5	14.9	39.3	55.21 γ^d_s : 28.93 γ^p_s : 26.28	20.16–21.92	40.09–43.70
M2 (2 %)	50.3	40.7	11.5	44.0	49.81 γ^d_s : 31.05 γ^p_s : 18.77	12.56–18.40	30.40–37.90
M2 (8 %)	36.5	31.5	2.0	33.9	62.18 γ^d_s : 38.94 γ^p_s : 23.25	21.12–24.26	45.60–54.39

Table A2: SCA, SE (with disperse (γ^d_s), and polar (γ^p_s) components) and DCA results on the TS of float glass with the test fluid diiodomethane

Methods	Static contact angle measurements (2 μ l) [°]				Surface energy [mJ/m ²]	Dynamic contact angle measurements (diiodomethane)	
	Water	Diiodomethane	Benzyl alc.	Glycerol		Hysteresis [°]	Drop age [s]
EM	1.0	42.1	22.1	20.8	52.12 γ^d_s : 30.30 γ^p_s : 19.82	39.84–41.99	72.99–82.40
M1 (2 h)	23.1	36.5	15.0	31.3	60.92 γ^d_s : 27.74 γ^p_s : 33.18	17.96–22.54	37.89–41.30
M1 (4 h)	37.1	37.2	15.8	39.3	55.62 γ^d_s : 28.87 γ^p_s : 26.75	23.19–28.15	46.20–54.20
M1 (8 h)	22.2	36.1	10.3	39.4	59.89 γ^d_s : 27.23 γ^p_s : 32.65	26.66–30.09	44.70–51.39
M2 (2 %)	47.5	41.9	12.0	50.9	49.53 γ^d_s : 29.19 γ^p_s : 20.35	24.32–29.43	46.19–49.30
M2 (8 %)	34.9	33.1	2.0	33.4	62.29 γ^d_s : 37.83 γ^p_s : 24.46	16.95–20.73	39.19–41.70

Table A3: SCA, SE (with disperse (γ^d_s), and polar (γ^p_s) components) and DCA results on PE foil surface with the test fluid diiodomethane

Methods	Static contact angle measurements (2 μ l) [°]				Surface energy [mJ/m ²]	Dynamic contact angle measurements (diiodomethane)	
	Water	Diiodomethane	Benzyl alc.	Glycerol		Hysteresis [°]	Drop age [s]
PE foil	101.2	56.2	45.6	88.9	30.92 γ^d_s : 30.80 γ^p_s : 0.12	9.75–12.98	28.89–33.79

Table A4: SCA, SE (with disperse (γ^d_s), and polar (γ^p_s) components) and DCA results on the AS of float glass with the test fluid water

Methods	Static contact angle measurements (2 μ l) [°]				Surface energy [mJ/m ²]	Dynamic contact angle measurements (water)	
	Water	Diiodomethane	Benzyl alc.	Glycerol		Hysteresis [°]	Drop age [s]
EM	1.0	45.2	28.9	18.9	51.83 γ^d_s : 30.36 γ^p_s : 21.47	< 10	Not detectable
M1 (2 h)	41.1	35.3	14.7	36.6	54.92 γ^d_s : 30.78 γ^p_s : 24.14	18.20–24.08	51.39–53.69
M1 (4 h)	35.7	39.7	18.5	32.7	56.36 γ^d_s : 28.34 γ^p_s : 28.02	25.08–33.66	79.99–97.49
M1 (8 h)	37.8	37.5	14.9	39.3	55.21 γ^d_s : 28.93 γ^p_s : 26.28	21.88–27.54	61.00–75.40
M2 (2 %)	50.3	40.7	11.5	44.0	49.81 γ^d_s : 31.05 γ^p_s : 18.77	33.31–37.41	93.99–110.19
M2 (8 %)	36.5	31.5	2.0	33.9	62.18 γ^d_s : 38.94 γ^p_s : 23.25	24.23–29.31	62.19–73.49

Table A5: SCA, SE (with disperse (γ_s^d), and polar (γ_s^p) components) and DCA results on the TS of float glass with the test fluid water

Methods	Static contact angle measurements (2 μ l) [°]				Surface energy [mJ/m ²]	Dynamic contact angle measurements (water)	
	Water	Diiodomethane	Benzyl alc.	Glycerol		Hysteresis [°]	Drop age [s]
EM	1.0	42.1	22.1	20.8	52.12 γ_s^d : 30.30 γ_s^p : 19.82	< 10	Not detectable
M1 (2 h)	23.1	36.5	15.0	31.3	60.92 γ_s^d : 27.74 γ_s^p : 33.18	< 10	Not detectable
M1 (4 h)	37.1	37.2	15.8	39.3	55.62 γ_s^d : 28.87 γ_s^p : 26.75	32.62–38.14	90.30–102.29
M1 (8 h)	22.2	36.1	10.3	39.4	59.89 γ_s^d : 27.23 γ_s^p : 32.65	21.57–30.09	63.19–77.69
M2 (2 %)	47.5	41.9	12.0	50.9	49.53 γ_s^d : 29.19 γ_s^p : 20.35	39.19–43.15	114.89–130.39
M2 (8 %)	34.9	33.1	2.0	33.4	62.29 γ_s^d : 37.83 γ_s^p : 24.46	27.01–32.82	75.49–85.69